NASA CONTRACTOR REPORT

INPUT ADMITTANCE AND REFLECTION COEFFICIENT OF A CIRCULAR APERTURE IN A GROUND PLANE COVERED BY A HOMOGENEOUS DIELECTRIC OR PLASMA SLAB

by R. E. Van Doeren

Prepared by
OHIO STATE UNIVERSITY
Columbus, Ohio
for

NATIONAL AERONAUTICS AND SPACE ADMINISTRATION • WASHINGTON, D. C. • SEPTEMBER 1968

NASA CR-1177

INPUT ADMITTANCE AND REFLECTION COEFFICIENT OF A CIRCULAR APERTURE IN A GROUND PLANE COVERED BY A HOMOGENEOUS DIELECTRIC OR PLASMA SLAB

By R. E. Van Doeren

Prepared under Grant No. NGR-36-008-048 by
OHIO STATE UNIVERSITY
Columbus, Ohio

for

NATIONAL AERONAUTICS AND SPACE ADMINISTRATION

For sale by the Clearinghouse for Federal Scientific and Technical Information
Springfield, Virginia 22151 – CFSTI price $3.00

ABSTRACT

This report is concerned with the reflection coefficient and admittance of a circular aperture in a ground plane radiating into a dielectric slab medium lying directly on the ground plane. The work relies heavily on previous efforts by Compton[1] and Rudduck.[6] Calculations are performed for lossless dielectric and lossy plasma slabs. The admittance for lossless slabs is compared with the experimental data of others.

TABLE OF CONTENTS

INPUT ADMITTANCE AND REFLECTION COEFFICIENT OF A CIRCULAR APERTURE IN A GROUND PLANE COVERED BY A HOMOGENEOUS DIELECTRIC OR PLASMA SLAB

I. INTRODUCTION

In this report an integral expression is found for the aperture admittance of a circular aperture in a ground plane covered by a homogeneous plasma or other dielectric slab. Interest in this research arose from a need for understanding the effects of re-entry plasma on circular-aperture antennas and for use in correlating reflectometer data from actual re-entry flights with homogeneous plasma slab parameters.

The method of analysis is variational and is based heavily on the original work by Compton[1] and Rudduck.[6] The basic variational assumption made in this case is that the functional form of the aperture electric field is that of the dominant TE_{11} mode for the aperture. Good agreement is obtained with experimental results obtained by others for nearly lossless Vycor ($\epsilon = 3.76$) slabs.

In Section II the admittance integral for the circular aperture is derived. Section III discusses the problems involved in numerically evaluating the integral and Section IV presents the numerical results for lossless dielectric slabs and for lossy plasmas with electron densities from zero to well-beyond plasma resonance. Section V presents the conclusions and Appendix A the derivation of the plane wave spectra for the circular aperture.

II. DERIVATION OF THE ADMITTANCE INTEGRAL FOR THE CIRCULAR APERTURE

In this section the derivation of a stationary expression for the admittance of an aperture in a ground plane is outlined. The procedure is that of Compton[1] and Rudduck.[6] The expression found is based on a stationary formula for the aperture admittance[2] and the simplifying assumption is made that the functional form of the fields in the aperture is that of the dominant mode for the aperture geometry. For the case of the circular aperture, this dominant mode is the TE_{11} mode.

The geometry of the problem is shown in Fig. 1.

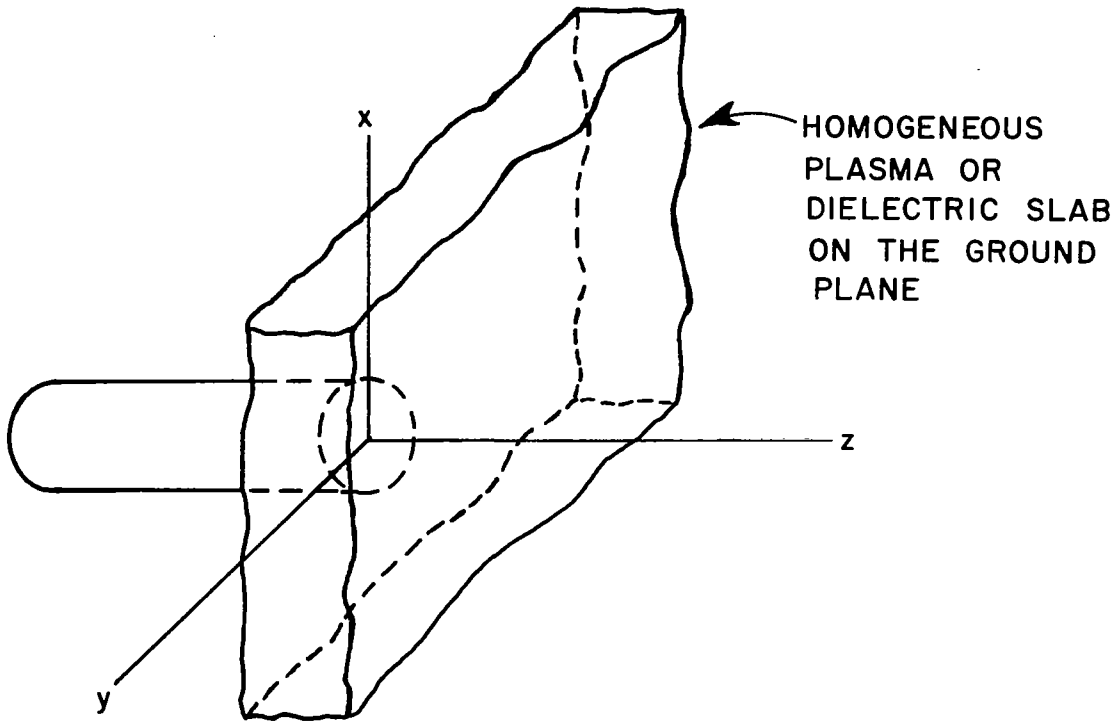

Fig. 1. Geometry of the circular aperture covered by a slab.

Space beyond the aperture plane is divided into two regions, as shown in Fig. 2.

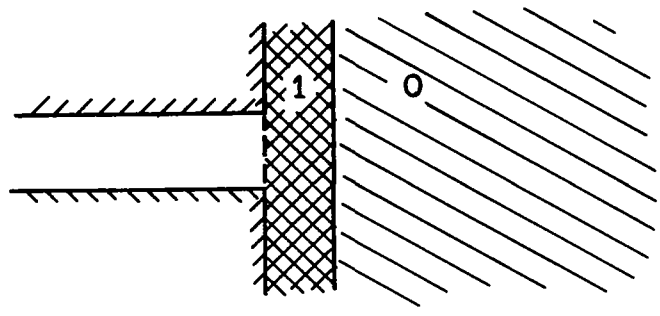

Fig. 2. Regions of space.

The fields outside the aperture are expressed in terms of the electric vector potential as follows:

$$(1)\qquad \begin{cases} \underline{E} = -\nabla \times \underline{F} \\ H = \dfrac{1}{j\omega \mu_o} \left[\nabla(\nabla \cdot \underline{F}) + k_{1,0}^2 \, \underline{F} \right] \end{cases}$$

and

$$(2)\qquad \underline{F} = \hat{x}\,\Phi + \hat{y}\,\Psi \quad .$$

$k_{1,0}$ is the free space propagation constant in regions 1 or 0, respectively. Φ and Ψ satisfy the scalar Helmholtz equation[3] in the two regions outside the aperture and can be expressed as Fourier integrals in those regions as follows (subscripts identify the regions):

$$(3)\qquad \begin{cases} \Phi_1(x, y, z) = \dfrac{1}{(2\pi)^2} \displaystyle\int_{-\infty}^{\infty}\int_{-\infty}^{\infty} \left[I_\Phi \, e^{-jk_{z1}z} + R_\Phi \, e^{+jk_{z1}z} \right] e^{-jk_x x} \, e^{-jk_y y} \cdot dk_x \, dk_y \\ \Psi_1(x, y, z) = \dfrac{1}{(2\pi)^2} \displaystyle\int_{-\infty}^{\infty}\int_{-\infty}^{\infty} \left[I_\Psi \, e^{-jk_{z1}z} + R_\Psi \, e^{+jk_{z1}z} \right] e^{-jk_x x} \, e^{-jk_y y} \cdot dk_x \, dk_y \\ \Phi_0(x, y, z) = \dfrac{1}{(2\pi)^2} \displaystyle\int_{-\infty}^{\infty}\int_{-\infty}^{\infty} T_\Phi \, e^{-jk_{z0}z} \, e^{-jk_x x} \, e^{-jk_y y} \, dk_x \, dk_y \\ \Psi_0(x, y, z) = \dfrac{1}{(2\pi)^2} \displaystyle\int_{-\infty}^{\infty}\int_{-\infty}^{\infty} T_\Psi \, e^{-jk_{z0}z} \, e^{-jk_x x} \, e^{-jk_y y} \, dk_x \, dk_y \quad . \end{cases}$$

Application of the scalar Helmholtz equation to Eq. (3) gives the following forms for k_{z1} and k_{z0}:

$$(4)\qquad \begin{cases} k_{z1} = \pm \sqrt{k_1^2 - (k_x^2 + k_y^2)} \\ k_{z0} = \pm \sqrt{k_0^2 - (k_x^2 + k_y^2)} \end{cases}$$

It is important to note that satisfaction of the radiation condition (the fields must approach zero as $z \to \infty$) requires that $\mathrm{Im}(k_{z1}) < 0$ and $\mathrm{Im}(k_{z0}) < 0$ which necessitates choosing the sign of the square root carefully. The time dependence $\exp(+j\omega t)$ is understood throughout.

The fields in both regions are found by applying Eq. (1) to Eq. (3) to get

$$(5)\quad E_{x1}(x, y, z) = \frac{1}{(2\pi)^2} \int_{-\infty}^{\infty}\int_{-\infty}^{\infty} \left[-jk_{z1} I_\Psi e^{-jk_{z1}z} + jk_{z1} R_\Psi e^{+jk_{z1}z}\right] \cdot e^{-jk_x x} e^{-jk_y y}\, dk_x\, dk_y ,$$

$$(6)\quad E_{y1}(x, y, z) = \frac{1}{(2\pi)^2} \int_{-\infty}^{\infty}\int_{-\infty}^{\infty} \left[jk_{z1} I_\Phi e^{-jk_{z1}z} - jk_{z1} R_\Phi e^{+jk_{z1}z}\right] \cdot e^{-jk_x x} e^{-jk_y y}\, dk_x\, dk_y ,$$

$$(7)\quad H_{x1}(x, y, z) = \frac{1}{(2\pi)^2} \int_{-\infty}^{\infty}\int_{-\infty}^{\infty} \left\{\frac{k_1^2 - k_x^2}{j\omega\mu_o}\left[I_\Phi e^{-jk_{z1}z} + R_\Phi e^{+jk_{z1}z}\right] - \frac{k_x k_y}{j\omega\mu_o}\left[I_\Psi e^{-jk_{z1}z} + R_\Psi e^{+jk_{z1}z}\right]\right\} e^{-jk_x x} e^{-jk_y y}\, dk_x\, dk_y ,$$

$$(8)\quad H_{y1}(x, y, z) = \frac{1}{(2\pi)^2} \int_{-\infty}^{\infty}\int_{-\infty}^{\infty} \left\{\frac{k_1^2 - k_y^2}{j\omega\mu_o}\left[I_\Psi e^{-jk_{z1}z} + R_\Psi e^{+jk_{z1}z}\right] - \frac{k_x k_y}{j\omega\mu_o}\left[I_\Phi e^{-jk_{z1}z} + R_\Phi e^{+jk_{z1}z}\right]\right\} e^{-jk_x x} e^{-jk_y y}\, dk_x\, dk_y ,$$

$$(9)\quad E_{x0}(x, y, z) = \frac{1}{(2\pi)^2} \int_{-\infty}^{\infty}\int_{-\infty}^{\infty} -jk_{z0} T_\Psi e^{-jk_{z0}z} e^{-jk_x x} e^{-jk_y y}\, dk_x\, dk_y ,$$

$$(10)\quad E_{y0}(x, y, z) = \frac{1}{(2\pi)^2} \int_{-\infty}^{\infty}\int_{-\infty}^{\infty} jk_{z0} T_\Phi e^{-jk_{z0}z} e^{-jk_x x} e^{-jk_y y}\, dk_x\, dk_y ,$$

$$(11)\quad H_{x0}(x, y, z) = \frac{1}{(2\pi)^2} \int_{-\infty}^{\infty}\int_{-\infty}^{\infty} \left[\frac{k_0^2 - k_x^2}{j\omega\mu_0} T_\Phi - \frac{k_x k_y}{j\omega\mu_0} T_\Psi \right] \cdot e^{-jk_{z0}z} e^{-jk_x x} e^{-jk_y y}\, dk_x\, dk_y ,$$

and

$$(12)\quad H_{y0}(x, y, z) = \frac{1}{(2\pi)^2} \int_{-\infty}^{\infty}\int_{-\infty}^{\infty} \left[\frac{k_0^2 - k_y^2}{j\omega\mu_0} T_\Psi - \frac{k_x k_y}{j\omega\mu_0} T_\Phi \right] \cdot e^{-jk_{z0}z} e^{-jk_x x} e^{-jk_y y}\, dk_x\, dk_y .$$

In order to find the aperture magnetic field, (the electric field is assumed), it is necessary to apply the boundary conditions on tangential $\underline{E}$ and $\underline{H}$ at z = d and on tangential $\underline{E}$ at z = 0. This can be accomplished by equating the integrands (spectra) of the tangential components at z = 0 and z = d. The assumption of the electric fields in the aperture allows use of the Fourier transform pair relations to find the spectrum of the electric field at z = 0. At z = 0, we have

$$(13)\quad \begin{cases} E_x(x, y, 0) = \dfrac{1}{(2\pi)^2} \displaystyle\int_{-\infty}^{\infty}\int_{-\infty}^{\infty} f_\Psi\, e^{-jk_x x} e^{-jk_y y}\, dk_x\, dk_y \\ E_y(x, y, 0) = \dfrac{1}{(2\pi)^2} \displaystyle\int_{-\infty}^{\infty}\int_{-\infty}^{\infty} f_\Phi\, e^{-jk_x x} e^{-jk_y y}\, dk_x\, dk_y \end{cases}$$

and

$$(14)\quad \begin{cases} f_\Psi(k_x, k_y) = \displaystyle\int_{-\infty}^{\infty}\int_{-\infty}^{\infty} E_x(x, y, 0)\, e^{+jk_x x} e^{+jk_y y}\, dx\, dy \\ f_\Phi(k_x, k_y) = \displaystyle\int_{-\infty}^{\infty}\int_{-\infty}^{\infty} E_y(x, y, 0)\, e^{+jk_x x} e^{+jk_y y}\, dx\, dy \end{cases} .$$

Here, f_Ψ and f_Φ are the spectra of the aperture field; these spectra are evaluated in Appendix A for the case when the aperture fields are those of the TE_{11} mode.

The boundary conditions at $z = 0$ require

$$jk_{z1}(-I_\Psi + R_\Psi) = f_\Psi \tag{15}$$

and

$$jk_{z1}(I_\Phi - R_\Phi) = f_\Phi \quad . \tag{16}$$

Application of the boundary condition at $z = d$ gives

$$-jk_{z1}\left[I_\Psi\, e^{-jk_{z1}d} - R_\Psi\, e^{+jk_{z1}d}\right] = -\,jk_{z0}\, T_\Psi\, e^{-jk_{z0}d} \tag{17}$$

$$jk_{z1}\left[I_\Phi\, e^{-jk_{z1}d} - R_\Phi\, e^{+jk_{z1}d}\right] = jk_{z0}\, T_\Phi\, e^{-jk_{z0}d} \quad , \tag{18}$$

$$\begin{aligned}(k_1^2 - k_x^2)\left[I_\Phi\, e^{-jk_{z1}d} + R_\Phi\, e^{+jk_{z1}d}\right] \\ - k_x k_y \left[I_\Psi\, e^{-jk_{z1}d} + R_\Psi\, e^{+jk_{z1}d}\right] \\ = \left[(k_0^2 - k_x^2)\, T_\Phi - k_x k_y\, T_\Psi\right] e^{-jk_{z0}d} \quad ,\end{aligned} \tag{19}$$

and

$$\begin{aligned}(k_1^2 - k_y^2)\left[I_\Psi\, e^{-jk_{z1}d} + R_\Psi\, e^{+jk_{z1}d}\right] \\ - k_x k_y \left[I_\Phi\, e^{-jk_{z1}d} + R_\Phi\, e^{+jk_{z1}d}\right] \\ = \left[(k_0^2 - k_y^2)\, T_\Psi - k_x k_y\, T_\Phi\right] e^{-jk_{z0}d}\end{aligned} \tag{20}$$

The six linear equations can then be solved for I_Ψ, R_Ψ and I_Φ and R_Φ by the method of determinants. The solution is clear cut except for the case of a slab dielectric constant with no imaginary part. In this instance, there exist zeros of the coefficient determinant for certain values of $(k_x^2 + k_y^2)$ which correspond to surface wave modes excited in the slab. Section III discusses the effects of these zeros.

The stationary admittance formula derived by Compton[2] and which is basic to this analysis, is given below.

$$Y = \frac{\int\int_{\text{aperture}} \underline{E}(x, y, 0) \times \underline{\Gamma}(x, y) \cdot \hat{z}\, dxdy}{\left[\int\int_{\text{aperture}} \underline{E}(x, y, 0) \cdot \overline{e}_o(x, y) dxdy\right]^2} \tag{21}$$

and

$$\underline{\Gamma}(x, y) = \underline{H}(x, y, 0) + \sum_{n=1}^{\infty} Y_n \underline{h}_n(x, y) \int\int_{\text{aperture}} \underline{E}(n, \xi, 0) \cdot \underline{e}_n(n, \xi)\, dnd\xi\,, \tag{22}$$

where $\underline{E}(x, y, 0)$ and $\underline{H}(x, y, 0)$ are the electric and magnetic fields in the aperture, $\underline{e}_n(x, y)$ and $\underline{h}_n(x, y)$ are the transverse vector mode functions[4] suitable for the aperture geometry of interest, and Y_n is the n-th mode characteristic admittance of a waveguide with the same cross section as the aperture.

The aperture electric field is taken to be normalized and to be of the dominant mode form; hence, the denominator of Eq. (2) is unity. Because of the orthogonality of the vector mode functions, the numerator simplifies to the following:

$$Y = \int\int_{\text{aperture}} \underline{E}(x, y, 0) \times \underline{H}(x, y, 0) \cdot \hat{z}\, dxdy\,. \tag{23}$$

Because tangential $\underline{E}$ is zero everywhere in the aperture plane except over the aperture, it is valid to extend the integration over all x, y space:

$$(24) \qquad Y = \int_{-\infty}^{\infty}\int_{-\infty}^{\infty} \underline{E}(x, y, 0) \times \underline{H}(x, y, 0) \cdot \hat{z}\, dxdy \quad .$$

If there are both $\hat{x}$ and $\hat{y}$ components of $\underline{E}$ and $\underline{H}$, Eq. (24) becomes

$$(25) \qquad Y = \int_{-\infty}^{\infty}\int_{-\infty}^{\infty} [\, E_x(x, y, 0)\, H_y(x, y, 0) - E_y(x, y, 0)\, H_x(x, y, 0)]\, dxdy \quad .$$

Parseval's theorem can be applied to the above formula to give an equation for the admittance in terms of the spectra of the field components;[5] i.e.,

$$(26) \qquad Y = \frac{1}{(2\pi)^2}\int_{-\infty}^{\infty}\int_{-\infty}^{\infty} \left\{ [-jk_{z1}(I_\Psi - R_\Psi)] * \left[\frac{k_1^2 - k_y^2}{j\omega\mu_o}(I_\Psi + R_\Psi) - \frac{k_x k_y}{j\omega\mu_o}(I_\Phi + R_\Phi) \right] \right.$$

$$\left. - [jk_{z1}(I_\Phi - R_\Phi)] * \left[\frac{k_1^2 - k_x^2}{j\omega\mu_o}(I_\Phi + R_\Phi) - \frac{k_x k_y}{j\omega\mu_o}(I_\Psi + R_\Psi) \right] \right\} dk_x dk_y \quad .$$

We now use Eqs. (15) and (16) to express R_Ψ in terms of I_Ψ and R_Φ in terms of I_Φ. The following form for Y results (f_Ψ and f_Φ are real):

$$(27) \quad Y = \frac{-j}{\omega\mu_o(2\pi)^2}\int_{-\infty}^{\infty}\int_{-\infty}^{\infty} \left\{ 2[(k_1^2 - k_y^2) f_\Psi + k_x k_y f_\Phi]\, I_\Psi - 2[(k_1^2 - k_x^2) f_\Phi + k_x k_y f_\Psi]\, I_\Phi \right.$$

$$\left. + \frac{1}{jk_{z1}} [f_\Psi^2 (k_1^2 - k_y^2) + f_\Phi^2 (k_1^2 - k_x^2) + 2 f_\Psi f_\Phi k_x k_y] \right\} dk_x\, dk_y \quad .$$

The above integration can be reduced to one finite and one infinite integral by the following change of variables:

(28)
$$
\begin{cases}
\eta = \dfrac{k_x}{k_0} = \beta \cos\alpha \\
\xi = \dfrac{k_y}{k_0} = \beta \sin\alpha \\
dk_x dk_y = k_0^2 \, \beta \, d\alpha \, d\beta \\
k_0 = \omega\sqrt{\mu_0 \epsilon_0} \\
k_1 = \omega\sqrt{\mu_0 \epsilon_1} \\
R = \dfrac{k_{z1}}{k_0} \\
P = \dfrac{k_{z0}}{k_0} \\
\rho = \dfrac{k_1}{k_0} = c\, e^{-j\frac{\phi}{2}} \\
F_\Psi = k_0 f_\Psi \\
F_\Phi = k_0 f_\Phi
\end{cases}
$$

When Eqs. (28) and (29) are substituted into Eq. (27), the final result for the admittance is

(29)
$$
Y = Y_0 \left(\frac{-j}{4\pi^2}\right) \int_0^{2\pi} \int_0^{\infty} \Bigg\{ 2\left[F_\Psi(\rho^2 - \beta^2 \sin^2\alpha) + F_\Phi \frac{\beta^2}{2} \sin 2\alpha\right] I_\Psi' - 2\left[F_\Phi(\rho^2 - \beta^2 \cos^2\alpha) + F_\Psi \frac{\beta^2}{2} \sin 2\alpha\right] I_\Phi' - j\frac{1}{R}\left[F_\Psi^2(\rho^2 - \beta^2 \sin^2\alpha) + F_\Phi^2(\rho^2 - \beta^2 \cos^2\alpha) + F_\Psi F_\Phi \beta^2 \sin 2\alpha\right] \Bigg\} \beta \, d\beta \, d\alpha,
$$

and $Y_0 = \sqrt{\epsilon_0/\mu_0}$ is the characteristic admittance of free space.

For the case in which the medium beyond the aperture is semi-infinite in extent, there will be no reflected waves in the medium and Eqs. (15) and (16), with $R_\Psi = 0$ and $R_\Phi = 0$, can be substituted into Eq. (29) to obtain the following admittance integral for a semi-infinite medium beyond the aperture:

$$(30)\quad Y = Y_o \left(\frac{-j}{4\pi^2}\right) \int_0^{2\pi} \int_0^{\infty} \frac{j}{R} \{(\rho^2 - \beta^2 \sin^2\alpha)F_\Psi^2 + (\rho^2 - \beta^2\cos^2\alpha)F_\Phi^2 + \beta^2 \sin 2\alpha\, F_\Psi F_\Phi\}\, \beta\, d\beta\, d\alpha$$

III. NUMERICAL EVALUATION OF THE INTEGRAL

Integration of Eq. (29) is accomplished in a straightforward manner except for the appearance of singularities (poles) of the integrand when the slab dielectric constant is pure real. These poles correspond to values of β for which surface-wave modes are excited in the slab.[6]

The poles are actually zeros of the determinant of the coefficients of the set of simultaneous equations in I_Ψ, I_Φ, R_Ψ, R_Φ, T_Ψ, and T_Φ. This determinant appears in the denominator of the solutions of I_Ψ and I_Φ and thus its zeros give rise to poles of the integrand. The occurrence of these poles and the method of handling them for the lossless dielectric slab are discussed in detail by Rudduck.[6] Although the problem Rudduck considers is that of the rectangular aperture, the system of equations for the scalar potential functions is identical to that for the circular aperture and the pole locations and behavior are therefore the same also.

The coefficient determinant can be factored to get the denominator in the solution for I_Ψ and I_Φ in the following form:

$$(31)\quad DEN = -jRP(j\rho^2 P^2 \cos RD - R \sin RD)(j P \sin RD + R \cos RD)\,,$$

where

$$P = \begin{cases} \sqrt{1 - \beta^2} & \beta^2 \le 1 \\ -j\sqrt{\beta^2 - 1} & \beta^2 > 1 \end{cases},$$

$$R = \begin{cases} \sqrt{\rho^2 - \beta^2} & \beta^2 \le \rho^2 \\ -j\sqrt{\beta^2 - \rho^2} & \beta^2 > \rho^2 \end{cases} \qquad (\rho^2 \text{ positive real})\,,$$

$$\rho = c\, e^{-j\frac{\phi}{2}} = \sqrt{\epsilon} \quad ,$$

and

$$\epsilon = \epsilon' + j\,\epsilon'' \quad \text{(relative slab permittivity)}.$$

The correct branches of P and R have been chosen to satisfy the radiation condition. In the equation for R, ρ^2 has been taken positive real in order to demonstrate the choice of the correct branch. For ρ^2 negative real ($\rho^2 = -|\epsilon'|$, as for a plasma), the following choice of R must be made:

$$R = -j\sqrt{|\epsilon'| + \beta^2} \quad .$$

As pointed out by Rudduck, the zeros of the denominator can be related to either TE or TM modes, depending on which denominator factor goes to zero. Reference to Collin[7] allows identification of the zeros of the two factors as corresponding to either odd TE or even TM surface-wave modes. There are no poles for $c \leq 1$. The two equations which β must satisfy in order to have these zeros are

$$\tan\left(2\pi\,\frac{d}{\lambda}\,\sqrt{\rho^2 - \beta^2}\right) = -\frac{\sqrt{\rho^2 - \beta^2}}{\sqrt{\beta^2 - 1}} \qquad \text{(TE modes)} \tag{32}$$

and

$$\tan\left(2\pi\,\frac{d}{\lambda}\,\sqrt{\rho^2 - \beta^2}\right) = \frac{\rho^2\sqrt{\beta^2 - 1}}{\sqrt{\rho^2 - \beta^2}} \qquad \text{(TM modes)} \quad . \tag{33}$$

These equations are given by Rudduck[6] and are applied to the case of the lossless dielectric slab. It can be shown for ρ^2 positive real, poles can occur only for $1.0 < \beta < c$. For such a case, the procedure followed is to accurately locate the poles numerically and then to numerically integrate very close up to, between, and beyond the poles and then to use residue theory[8] to account for a small clockwise excursion taken around each pole. The same procedure is followed for the TM plasma slab pole discussed later.

Figure 3 shows a sketch of the contour of integration used for the lossless slab for the case in which there are two poles. For lossy slab media, the poles move off the real β-axis and have a negative imaginary part; the semi-circular excursion is therefore taken in the upper

half-plane to ensure continuity of the results as the slab changes from lossy to lossless.

The value of the integral around the clockwise semi-circular excursion is equal to $(-j\pi)$ times the residue of the pole.

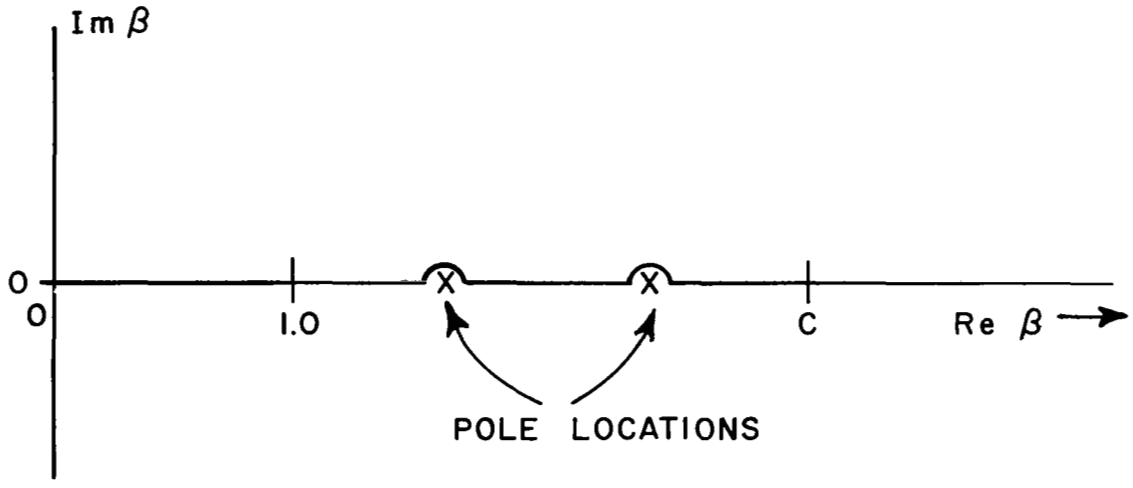

Fig. 3. Sketch of contour of integration for a lossless slab.

As is evident from Eqs. (32) and (33) a multiplicity of poles is possible for the case of a lossless dielectric slab with a positive real dielectric constant; for a negative real dielectric constant (e.g., for a plasma) the situation is altered. In this case, only one pole, corresponding to a TM surface-wave mode can exist and this pole can be found anywhere from $\beta > 1$ to $\beta \to \infty$.

For the case of a plasma slab, the effective dielectric constant can be expressed as follows:[9]

$$\epsilon = \left(1 - \frac{\omega_p^2}{\omega^2 + \nu^2}\right) - j\,\frac{\nu}{\omega}\,\frac{\omega_p^2}{\omega^2 + \nu^2} = \epsilon' + j\epsilon'' \,, \tag{34}$$

where

ω is 2π times the oscillation frequency (sec^{-1}) ,

ν is the electron collision frequency (sec^{-1}) ,

ω_p is the plasma collision frequency:

$$\omega_p = (5.66 \times 10^4)(N_e)^{\frac{1}{2}} \quad (\text{sec}^{-1}), \text{ and}$$

N_e is the electron density in cm^{-3} .

Consideration of Eq. (34) makes it evident that the real part of the effective plasma dielectric constant is always less than unity and can become an arbitrarily large negative number as N_e becomes arbitrarily large. At the plasma resonance ($\omega_p^2 = \omega^2 + \nu^2$), the real part vanishes. The electron density which produces this condition is often called the "cutoff" concentration.

The pole locations for plasmas with $c > 1$ are found by taking $\phi = \pi(\epsilon'' = 0)$ and examining Eqs. (32) and (33) for $\rho^2 = -|\epsilon'|$ and $|\epsilon'| > 1$.

TE Surface Waves

$$\tan\left(2\pi \frac{d}{\lambda} \sqrt{\rho^2 - \beta^2}\right) = -\frac{\sqrt{\rho^2 - \beta^2}}{\sqrt{\beta^2 - 1}} \tag{35}$$

For $\rho^2 = -|\epsilon'|$, Eq. (35) becomes, after selection of the correct branch for $R = \sqrt{\rho^2 - \beta^2}$),

$$\tan\left(-j\, 2\pi \frac{d}{\lambda} \sqrt{|\epsilon'| + \beta^2}\right) = +j \frac{\sqrt{|\epsilon'| + \beta^2}}{\sqrt{\beta^2 - 1}} \quad . \tag{36}$$

We can write the tangent of the pure imaginary quantity above as follows:

$$\tan\left(-j\, 2\pi \frac{d}{\lambda} \sqrt{|\epsilon'| + \beta^2}\right) = -j \frac{e^{-2\pi \frac{d}{\lambda}\sqrt{|\epsilon'| + \beta^2}} - e^{+2\pi \frac{d}{\lambda}\sqrt{|\epsilon'| + \beta^2}}}{e^{-2\pi \frac{d}{\lambda}\sqrt{|\epsilon'| + \beta^2}} + e^{+2\pi \frac{d}{\lambda}\sqrt{|\epsilon'| + \beta^2}}} \tag{37}$$

For $|\epsilon'| > 1$, Eq. (37) gives a function which is negative imaginary for all β and monotone decreasing with β; its lower bound is $-j$. The right side of Eq. (36) is always positive imaginary for $\beta > 1$. Hence, there are no solutions to Eq. (36) and no TE surface-wave modes are excited for $\rho^2 = -|\epsilon'|$, $|\epsilon'| > 1$.

TM Surface Waves

$$(38) \qquad \tan\left(2\pi \frac{d}{\lambda} \sqrt{\rho^2 - \beta^2}\right) = \frac{\rho^2 \sqrt{\beta^2 - 1}}{\sqrt{\rho^2 - \beta^2}} \quad .$$

For $\rho^2 = -|\epsilon'|$, Eq. (38) becomes

$$(39) \qquad \tan\left(-j\, 2\pi \frac{d}{\lambda} \sqrt{|\epsilon'| + \beta^2}\right) = -j \frac{|\epsilon'| \sqrt{\beta^2 - 1}}{\sqrt{|\epsilon'| + \beta^2}} \quad .$$

The previous discussion of the left side of Eq. (36) applies to the left side of Eq. (39) also. For $\beta > 1$, the right side of Eq. (39) is monotone decreasing with β; its lower bound is $-j|\epsilon'|$. Thus there is a (single) solution to Eq. (39). Figure 4 shows a sketch of the behavior of the two sides of Eq. (39) for $\beta \geq 1$.

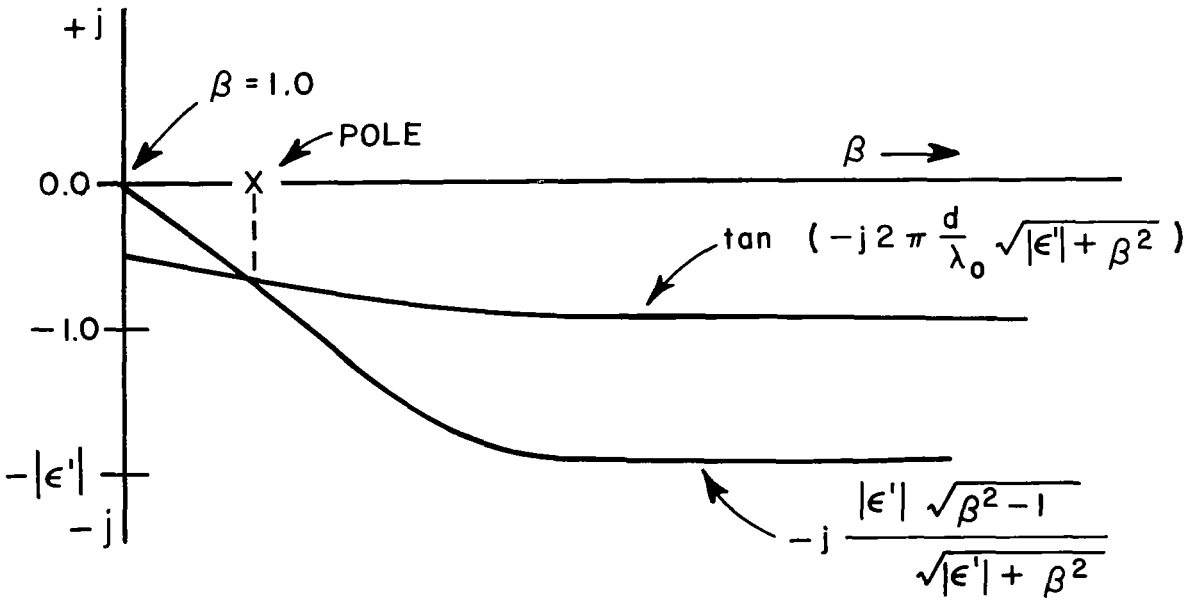

Fig. 4. Sketch showing the TM pole location for $|\epsilon'| > 1$.

In order to determine the possible range of values of β for this pole, we can consider the case for $2\pi\ d/\lambda$ sufficiently large that the left side of Eq. (39) is very nearly equal to $(-j)$ for the entire range of β. Then the pole location is determined by setting the right hand side of Eq. (39) equal to $(-j)$ and solving for β. The resulting equation for β is

$$\beta = \sqrt{\frac{|\epsilon'|}{|\epsilon'| - 1}} \quad . \tag{40}$$

As $|\epsilon'|$ becomes larger, the pole moves closer to $\beta = 1$ and as $|\epsilon'|$ approaches unity (say for $|\epsilon'|$ only slightly larger than unity) the value of β can be made arbitrarily large. Thus, the pole location can extend from a value of β arbitrarily close to 1.0 to a value of β arbitrarily large.

IV. NUMERICAL RESULTS

Data were generated using the OSU IBM 7094 computer to evaluate the admittance integral. Both lossless dielectric and lossy plasma slabs were considered.

Lossless Slab Data

The first data calculated were for lossless Vycor glass slabs ($\epsilon = 3.76$) for which considerable experimental admittance data have been gathered by researchers at the NASA Research Center, Langley, Virginia.[10] Table I gives the measured admittance and the admittance calculated using the variational method described previously in this report.

TABLE I
MEASURED AND CALCULATED ADMITTANCE FOR 1.5" DIAMETER CIRCULAR APERTURE IN A 12" × 12" GROUND PLANE COVERED BY A 0.515" THICK LOSSLESS SLAB OF DIELECTRIC CONSTANT, $\epsilon = 3.76$

Frequency	Measured Admittance	Calculated Admittance
5.89 GHz	1.68 - j 0.57	1.76 - j 0.44
6.30 GHz	1.62 + j 0.0	1.50 + j 0.001
7.31 GHz	1.60 + j 0.50	1.61 + j 0.34
7.48 GHz	1.81 + j 1.03	1.65 + j 0.94

The data were read from a graph and, where necessary, interpolation between adjacent points was used to find the suitable experimental value. There is good agreement between the experimental and the theoretical results. The same NASA researchers have measured

the free-space aperture admittance also; however, for the cases compared, the conductance was in good agreement and the calculated susceptance was approximately equal in magnitude to that measured but of the opposite sign. This sign difference has not been resolved. The generally good agreement with experiment is considered to substantiate the theory and, consequently, data were generated for other dielectric and plasma parameters of interest.

Table II shows the calculated aperture admittance at 10.044 GHz of a 0.74" diameter circular aperture in a ground plane covered by a lossless Teflon slab of several thicknesses.

TABLE II
CALCULATED APERTURE ADMITTANCE AND REFLECTION COEFFICIENT OF A 0.74 INCH DIAMETER APERTURE COVERED BY LOSSLESS TEFLON SLABS OF GIVEN THICKNESSES AT A FREQUENCY OF 10.044 GHz

d (inches)	Admittance	Reflection Coefficient
0.000	1.76 + j 0.12	-.277 - j .031; $\|.279\| e^{j-173.6°}$
0.100	2.57 + j 1.04	-.483 - j .150; $\|.506\| e^{j(-162.7°)}$
0.200	4.02 + j 0.70	-.609 - j .055; $\|.612\| e^{j(-174.9°)}$
0.300	3.78 - j 0.60	-.588 + j .052; $\|.590\| e^{j175.0°}$
0.400	2.89 - j 0.53	-.495 + j .069; $\|.500\| e^{j172.1°}$
0.500	2.67 + j 0.16	-.456 - j .024; $\|.456\| e^{j(-177.0°)}$
0.600	3.34 + j 0.51	-.546 - j .053; $\|.548\| e^{j(174.4°)}$
0.700	3.62 - j 0.16	-.568 + j .153; $\|.568\| e^{j178.5°}$
0.800	3.08 - j 0.34	-.513 + j .041; $\|.515\| e^{j175.5°}$
∞	3.16 + j 1.04	$\|.559\| e^{j(-168.3°)}$

Figure 5 shows a Smith Chart plot of the Teflon slab data; the data are plotted in impedance coordinates. It is interesting to note the spiralling-in of the reflection coefficient to the half-space value.

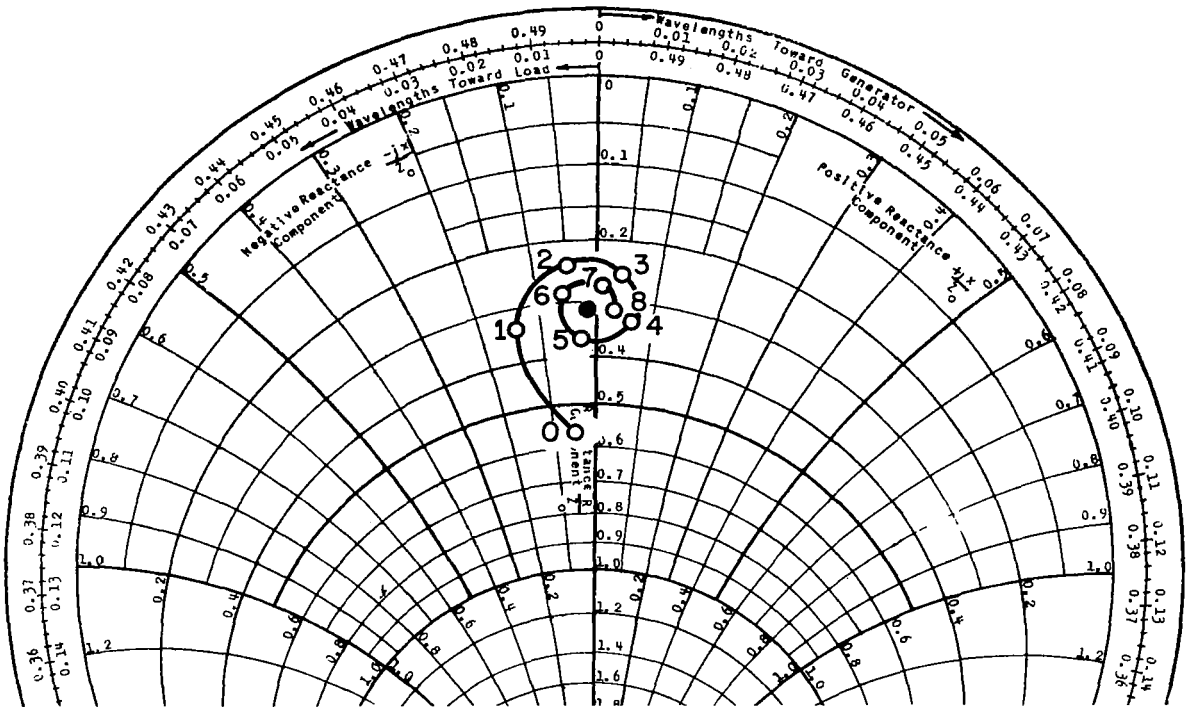

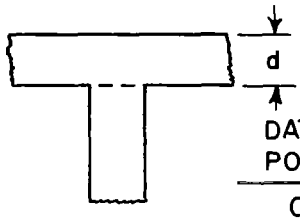

CIRCULAR APERTURE IMPEDANCE
APERTURE RADIUS 0.37"
LOSSLESS TEFLON LAYERS
FREQUENCY 10.044 GHz

DATA POINT	d (INCHES)
0	0.0 (FREE SPACE)
1	0.100
2	0.200
3	0.300
4	0.400
5	0.500
6	0.600
7	0.700
8	0.800
●	∞ (HALF-SPACE)

Fig. 5. Smith Chart plot of aperture impedance of a 0.74 inch diameter aperture covered by lossless teflon slab layers of thickness d at a frequency of 10.044 GHz.

Plasma Data

Admittance data were computed for aperture diameters of 0.74" at 10.044 GHz and 2.21" at 3.348 GHz when covered by homogeneous plasma slabs 0.197" and 0.788" thick and when radiating into a semi-infinite plasma half-space. The data were calculated for electron densities from zero to well beyond cutoff for a collision frequency equal to 10^8 sec^{-1}.

Table III shows the tabulated reflection coefficient data for 3.348 GHz and the range of electron densities considered. Figure 6 shows a Smith Chart presentation of the aperture impedance and reflection coefficient for the data presented in Table III.

Table IV gives the calculated reflection coefficient data for 10.044 GHz and the electron densities considered. Figure 7 is a Smith Chart presentation of the data from Table IV.

It is observed that the reflection coefficient curves converge to the minus unity value from the positive phase angle direction. This direction of approach to (-1) is consistent with plane wave theory for the homogeneous plasma medium. This can be seen if we write the characteristic impedance of the plasma medium in terms of the propagation constant in the plasma, k_p. Neglecting the collision frequency we find

$$z = \frac{\omega\mu_o}{k_p} = \frac{\omega\mu_o}{\omega\sqrt{\mu_o(-|\epsilon'|)}} = \frac{\omega\mu_o}{-j\omega\sqrt{\mu_o|\epsilon'|}}$$

and

$$z = j\sqrt{\frac{\mu_o}{|\epsilon'|}} \quad .$$

Thus, it is clear that as Ne $\rightarrow \infty$ (i.e., as $|\epsilon'| \rightarrow \infty$), $z \rightarrow 0$ on the positive reactance side of the Smith Chart. The correct branch for the propagation constant was chosen (i.e., $\mathrm{Im}(k_p) < 0$) in order to satisfy the radiation conditions.

TABLE III

REFLECTION COEFFICIENT OF A 2.21" DIAMETER APERTURE IN A GROUND PLANE COVERED BY A PLASMA SLAB OF THICKNESS d. 3.348 GHz

Data point (Fig. 6)	Electron density (cm^{-3})	Mag. ϵ	Arg. ϵ (rad.)	d = 0.197" Mag. Γ	d = 0.197" Arg. Γ (deg.)	d = 0.788" Mag. Γ	d = 0.788" Arg. Γ (deg.)	d = ∞ Mag. Γ	d = ∞ Arg. Γ (deg.)
0	0.0	1.0	0.000	0.291	-173.9°	0.291	-173.9°	0.291	-173.9°
1	5×10^{10}	0.638	-0.003	0.286	153.5	0.296	120.9	0.178	148.8
2	8×10^{10}	0.420	-0.007			0.473	108.4°	0.401	88.9
3	1.0×10^{11}	0.275	-0.013	0.327	128.2	0.615	109.0	0.674	93.7
4	1.2×10^{11}	0.130	-0.032			0.764	113.0	0.900	107.0
5	1.3×10^{11}	0.058	-0.077	0.497	108.9			0.968	114.1
6	1.6×10^{11}	0.160	-3.107	0.720	131.1			1.0	129.1
7	2.0×10^{11}	0.449	-3.126	0.780	140.8	0.973	138.7	1.0	138.4
8	8.0×10^{11}	4.79	-3.136	0.903	157.2	0.986	161.5	1.0	161.8
9	1.5×10^{12}	9.87	-3.136	0.973	164.7	0.994	167.0	1.0	167.0

TABLE IV

REFLECTION COEFFICIENT OF A 0.74" APERTURE IN A GROUND PLANE COVERED BY A PLASMA SLAB OF THICKNESS d. 10.044 GHz

Data point (Fig. 7)	Electron density (cm^{-3})	Mag. ϵ	Arg. ϵ (rad.)	d = 0.197" Mag. Γ	d = 0.197" Arg. Γ (deg.)	d = 0.788" Mag. Γ	d = 0.788" Arg. Γ (deg.)	d = ∞ Mag. Γ	d = ∞ Arg. Γ (deg.)
0	0.0	1.0	0.0	0.279	-173.6°	0.279	-173.6°	0.279	-173.6°
1	5.0×10^{11}	0.597	-0.001	0.306	123.3	0.189	107.4	0.206	110.0
2	8.0×10^{11}					0.581	81.6	0.531	87.2
3	1.0×10^{12}	0.195	-0.007	0.616	110.0	0.859	100.3	0.811	98.3
4	1.2×10^{12}	0.034	-0.045	0.810	114.7	0.977	115.4	0.987	114.5
5	2.0×10^{12}	0.610	-3.137	0.956	140.6			1.0	140.7
6	5.0×10^{12}					0.992	157.4	1.0	157.4

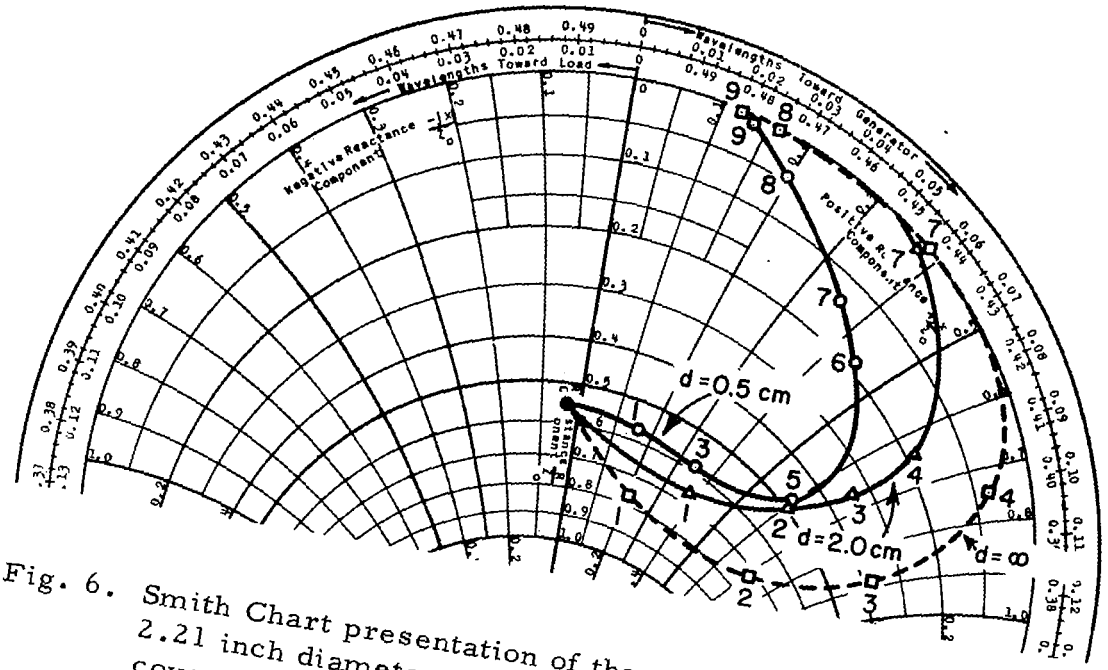

Fig. 6. Smith Chart presentation of the reflection coefficient of a 2.21 inch diameter circular aperture in a ground plane covered by a homogeneous plasma slab. The data points correspond to those listed in Table III. (3.348 GHz)

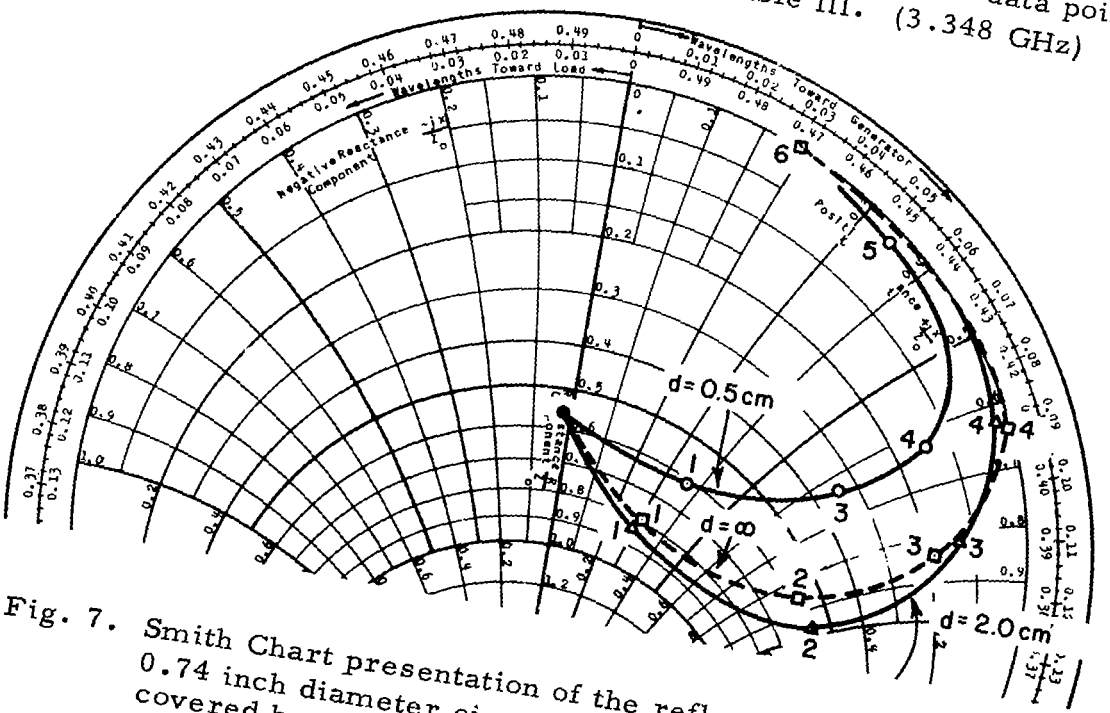

Fig. 7. Smith Chart presentation of the reflection coefficient of a 0.74 inch diameter circular aperture in a ground plane covered by a homogeneous plasma slab. The data points correspond to those listed in Table IV. (10.044 GHz)

V. CONCLUSIONS

The derivation of the variational solution for the admittance of an aperture in a ground plane covered by a homogeneous dielectric slab is reviewed. The formulation is extended to consideration of the circular aperture.

Numerical integration of the variational integral is discussed and the effects of poles of the integrand are considered. Admittance calculations were performed for lossless dielectric media and for plasma layers. Good agreement with experimental data obtained by others was found for the lossless dielectric calculations and the calculated plasma slab data were found to be generally consistent with expectations based on plane-wave reflection.

REFERENCES

1. Compton, R.T., Jr., "The Admittance of Aperture Antennas Radiating into Lossy Media," Report 1691-5, 15 March 1964, Antenna Laboratory, The Ohio State University Research Foundation; prepared under Grant Number NsG-448, National Aeronautics and Space Administration, Washington, D.C.

2. Ibid., p. 11

3. Harrington, R.F., Time Harmonic Electromagnetic Field, McGraw-Hill Book Co., New York, (1961), p. 38.

4. Ibid., p. 389.

5. Compton, loc. cit., p. 84.

6. Rudduck, R.C., "The Admittance of a Rectangular Waveguide Aperture Covered by a Lossless Dielectric Slab," Report 1691-22, 15 May 1967, ElectroScience Laboratory, The Ohio State University Research Foundation; prepared under Grant Number NsG-448, National Aeronautics and Space Administration, Wasington, D.C.

7. Collin, R.E., Field Theory of Guided Waves, McGraw-Hill Book Co., New York, pp. 470-474.

8. Phillips, E.G., "Functions of a Complex Variable," University Mathematical Texts, Interscience Publishers, Inc. (Oliver and Boyd, Ltd.), New York, Eighth Edition, Reprinted 1963, p. 121.

9. Holt, E.H. and R.E. Haskell, Foundation of Plasma Dynamics, The MacMillan Company, New York, (1965), p. 196.

10. Bailey, M.C. and C.T. Swift, "Input Admittance of a Circular Aperture Covered by a Dielectric Slab," Unpublished Report, (September 1967).

11. Silver, S., Microwave Antenna Theory and Design, Dover Publications, Inc., New York, p. 336-337.

APPENDIX A
PLANE WAVE SPECTRUM FOR THE TE_{11} CIRCULAR APERTURE

This derivation follows the steps outlined by Silver[11] in his derivation of the radiation field of the circular aperture.

The geometry is shown in Fig. 8.

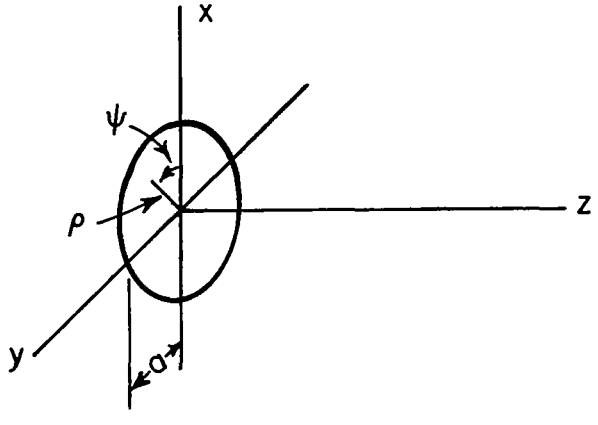

Fig. 8. Circular aperture geometry.

For the TE_{11} mode in the aperture, the electric scalar potential is given by

$$\Psi = N J_1(k_\rho \rho) \cos\psi \, e^{-jk_z z} \quad . \tag{41}$$

N is a normalization constant such that the denominator integral of Eq. (21) is equal to unity; i.e.,

$$\int_{\text{aperture}} \int \underline{E}(x, y, 0) \cdot \overline{e}_o(x, y) \, dx \, dy = 1$$

The electric vector potential is

$$\underline{F} = \hat{z} \, \Psi \tag{42}$$

and

$$\underline{E} = - \nabla \times \underline{F} \quad . \tag{43}$$

At $z = 0$,

$$\begin{cases} E_\rho = N \dfrac{J_1(k_\rho \rho)}{\rho} \sin \psi \\ E_\psi = N k_\rho \, J_1'(k_\rho \rho) \cos \psi \end{cases} \tag{44}$$

and

$$\begin{cases} E_x = E_\rho \cos \psi - E_\psi \sin \psi \\ E_y = E_\rho \sin \psi + E_\psi \cos \psi \end{cases} . \tag{45}$$

Then

$$\begin{cases} E_x = N \dfrac{J_1(k_\rho \rho)}{\rho} \sin \psi \cos \psi - N k_\rho J_1'(k_\rho \rho) \cos \psi \sin \psi \\ E_y = N \dfrac{J_1(k_\rho \rho)}{\rho} \sin^2 \psi + N k_\rho \, J_1'(k_\rho \rho) \cos^2 \psi \, , \end{cases} \tag{46}$$

but

$$\begin{cases} J_1'(z) = - \dfrac{1}{z} \, J_1(z) + J_0(z) \\ \dfrac{1}{z} J_1(z) = \dfrac{1}{2} \left[J_2(z) + J_0(z) \right] \end{cases} .$$

Thus

$$\begin{cases} E_x = N \dfrac{k_\rho}{2} \, J_2(k_\rho \rho) \sin 2\psi \\ E_y = N \dfrac{k_\rho}{2} \left[J_0(k_\rho \rho) - J_2(k_\rho \rho) \cos 2\psi \right] \end{cases} . \tag{47}$$

The Fourier transforms of E_x and E_y are defined as follows:

$$(48)\quad \begin{cases} f_\Psi = \int_{-\infty}^{\infty}\int_{-\infty}^{\infty} E_x(x, y, 0)\, e^{jk_x x}\, e^{jk_y y}\, dx\, dy \\ f_\Phi = \int_{-\infty}^{\infty}\int_{-\infty}^{\infty} E_y(x, y, 0)\, e^{jk_x x}\, e^{jk_y y}\, dx\, dy \end{cases} .$$

By making a change of variables as shown below, the transform can be written in cylindrical coordinates;

$$(49)\quad \begin{cases} x = \rho \cos\psi & k_x = k\cos\phi & k = k_o \sin\theta \\ y = \rho \sin\psi & k_y = k\sin\phi \end{cases} .$$

The geometrical interpretation of this change of variables is shown in Fig. 9.

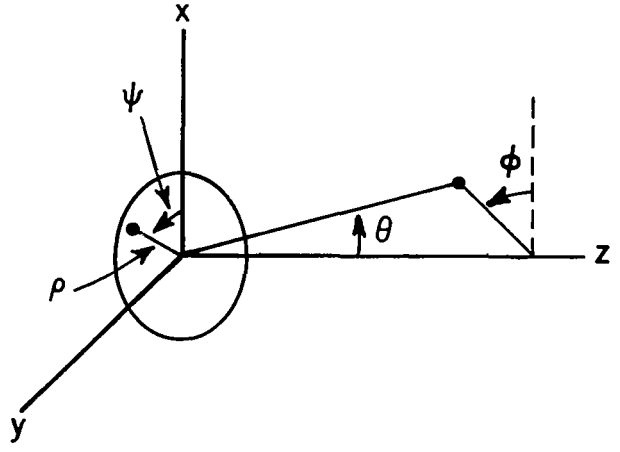

Fig. 9. Geometrical interpretation of the change of variables.

The integral transforms become

$$(50)\quad \begin{cases} f_\Psi = \int_0^a \int_0^{2\pi} E_x(\rho,\psi)\, e^{jk\rho[\cos\phi\cos\psi + \sin\phi\sin\psi]}\ \rho\, d\rho\, d\psi \\ f_\Phi = \int_0^a \int_0^{2\pi} E_y(\rho,\psi)\, e^{jk\rho[\cos\phi\cos\psi + \sin\phi\sin\psi]}\ \rho\, d\rho\, d\psi \end{cases} .$$

Substituting the assumed TE_{11} field in the integrals and simplifying the trigonometric details of the exponent, we find

$$(51)\quad \begin{cases} f_\Psi = N\frac{k\rho}{2} \int_0^a \int_0^{2\pi} J_2(k_\rho\rho)\sin 2\psi\ e^{j k_o\rho\sin\theta\cos(\phi-\psi)}\ \rho\, d\rho\, d\psi \\ f_\Phi = N\frac{k\rho}{2} \int_0^a \int_0^{2\pi} [J_o(k_\rho\rho) - J_2(k_\rho\rho)\cos 2\psi]\ e^{jk_o\rho\sin\theta\cos(\phi-\psi)}\ \rho\, d\rho\, d\psi \end{cases} .$$

In order to reduce the equations above, we need the relations given below.

The Fourier-Bessel Series

$$(52)\quad e^{j\lambda\rho\cos(\phi-\psi)} = J_o(\lambda\rho) + \sum_{m=1}^{\infty} 2(j)^m J_m(\lambda\rho)\cos m(\phi-\psi) .$$

The Lommel Integral Formula

$$(53)\quad \int_0^x x\, J_n(\alpha x)\, J_n(\beta x)\, dx = \frac{x}{\alpha^2-\beta^2}\left[J_n(\alpha x)\frac{d}{dx}J_n(\beta x) - J_n(\beta x)\frac{d}{dx}J_n(\alpha x)\right] .$$

When Eq. (52) is substituted into Eq. (51), a series of integrals over 2π of $(\sin 2\psi \cos m\psi)$ and $(\sin 2\psi \sin n\psi)$ result. The orthogonality properties of the sine and cosine functions eliminate consideration of any terms other than m = 0 and m = 2 in the Fourier-Bessel series. The result is

$$(54) \qquad f_\Psi = - N \frac{k_\rho}{2} \int_0^a \int_0^{2\pi} 2\, J_2(k_\rho \rho)\, J_2(k_o \rho \sin\theta) \sin 2\psi \cos 2(\phi - \psi)\, \rho\, d\rho\, d\psi$$

and

$$(55) \qquad f_\Phi = N \frac{k_\rho}{2} \int_0^a \int_0^{2\pi} \left[J_o(k_\rho \rho)\, J_o(k_o \rho \sin\theta) + 2\, J_2(k_\rho \rho)\, J_2(k_o \rho \sin\theta) \cos 2\psi \cos 2(\phi - \psi) \right] \rho\, d\rho\, d\psi \ .$$

Completion of the integration over ψ gives

$$(56) \qquad f_\Psi = - N k_\rho \pi \int_0^a \sin 2\phi\, J_2(k_\rho \rho)\, J_2(k_o \rho \sin\theta)\, \rho\, d\rho$$

and

$$(57) \qquad f_\Phi = N \pi k_\rho \int_0^a \left[J_o(k_\rho \rho)\, J_o(k_o \rho \sin\theta) + \cos 2\phi\, J_2(k_\rho \rho)\, J_2(k_o \rho \sin\theta) \right] \rho\, d\rho \ .$$

Application of the Lommel integral formula (Eq. (53)) gives as the final result for the transform of the TE_{11} aperture fields

$$(58) \qquad f_\Psi = N \frac{-\pi k_\rho a \sin 2\phi}{k_\rho^2 - k_o^2 \sin^2\theta} \left[k_o \sin\theta\, J_2(k_\rho a)\, J_2'(k_o a \sin\theta) - k_\rho\, J_2(k_o a \sin\theta)\, J_2'(k_\rho a) \right]$$

and

$$(59) \qquad f_\Phi = N \frac{\pi k_\rho a}{k_\rho^2 - k_o^2 \sin^2\theta} \left[\begin{array}{l} k_o \sin\theta\, J_o(k_\rho a)\, J_o'(k_o a \sin\theta) \\ - k_\rho\, J_o(k_o a \sin\theta)\, J_o'(k_\rho a) \\ + \cos 2\phi \left[k_o \sin\theta\, J_2(k_\rho a)\, J_2'(k_o a \sin\theta) \right. \\ \left. - k_\rho\, J_2(k_o a \sin\theta)\, J_2'(k_\rho a) \right] \end{array} \right].$$

For the TE_{11} mode, the normalization constant is given by Harrington[4] as

(60) $$N = \sqrt{\frac{2}{\pi[(1.841)^2 - 1]}} \; \frac{1}{J_1(1.841)} = 1.256 \quad .$$

After putting J_2' and J_0' in terms of J_1 and J_0, the final result for the plane-wave spectrum of the circular aperture is obtained, letting

(61) $$\begin{cases} A = k_0 A \\ F_\Psi = k_0 f_\Psi \\ F_\Phi = k_0 f_\Phi \\ \alpha = \phi \\ \beta = \sin\theta \quad , \end{cases}$$

(62) $$F_\Psi = \frac{A \sin 2\alpha}{(3.3899 - A^2\beta^2)} \left\{ \frac{10.993 - (1.621)A^2\beta^2}{A\beta} \cdot J_1(A\beta) - (5.496)\, J_0(A\beta) \right\} ,$$

and

(63) $$F_\Phi = \frac{A}{(3.3899 - A^2\beta^2)} \left\{ (5.496)(1 + \cos 2\alpha)\, J_0(A\beta) - \left[(1 - \cos 2\alpha)(1.621)A\beta + \frac{(5.496)\cos 2\alpha}{(\beta A)/2} \right] \cdot J_1(A\beta) \right\} .$$

"The aeronautical and space activities of the United States shall be conducted so as to contribute . . . to the expansion of human knowledge of phenomena in the atmosphere and space. The Administration shall provide for the widest practicable and appropriate dissemination of information concerning its activities and the results thereof."

— NATIONAL AERONAUTICS AND SPACE ACT OF 1958

NASA SCIENTIFIC AND TECHNICAL PUBLICATIONS

TECHNICAL REPORTS: Scientific and technical information considered important, complete, and a lasting contribution to existing knowledge.

TECHNICAL NOTES: Information less broad in scope but nevertheless of importance as a contribution to existing knowledge.

TECHNICAL MEMORANDUMS: Information receiving limited distribution because of preliminary data, security classification, or other reasons.

CONTRACTOR REPORTS: Scientific and technical information generated under a NASA contract or grant and considered an important contribution to existing knowledge.

TECHNICAL TRANSLATIONS: Information published in a foreign language considered to merit NASA distribution in English.

SPECIAL PUBLICATIONS: Information derived from or of value to NASA activities. Publications include conference proceedings, monographs, data compilations, handbooks, sourcebooks, and special bibliographies.

TECHNOLOGY UTILIZATION PUBLICATIONS: Information on technology used by NASA that may be of particular interest in commercial and other non-aerospace applications. Publications include Tech Briefs, Technology Utilization Reports and Notes, and Technology Surveys.

Details on the availability of these publications may be obtained from:

SCIENTIFIC AND TECHNICAL INFORMATION DIVISION

NATIONAL AERONAUTICS AND SPACE ADMINISTRATION

Washington, D.C. 20546